



## Article

# Synthesis of Phenol-Tagged Ruthenium Alkylidene Olefin Metathesis Catalysts for Robust Immobilisation Inside Metal–Organic Framework Support

Maryana Nadirova <sup>1</sup>, Joel Cejas-Sánchez <sup>1,2</sup> , Rosa María Sebastián <sup>2</sup> , Marcin Wiszniewski <sup>1</sup> , Michał J. Chmielewski <sup>1,\*</sup> , Anna Kajetanowicz <sup>1,\*</sup>  and Karol Grela <sup>1,\*</sup>

<sup>1</sup> Biological and Chemical Research Centre, Faculty of Chemistry, University of Warsaw, Żwirki i Wigury 101, 02-089 Warsaw, Poland

<sup>2</sup> Department of Chemistry and Centro de Innovación en Química Avanzada, Universitat Autònoma de Barcelona, Cerdanyola del Vallès, Bellaterra, 08193 Barcelona, Spain

\* Correspondence: mchmielewski@chem.uw.edu.pl (M.J.C.); a.kajetanowicz@uw.edu.pl (A.K.); kl.grela@uw.edu.pl (K.G.)

**Abstract:** Two new unsymmetrical N-heterocyclic carbene ligand (uNHC)-based ruthenium complexes featuring phenolic OH function were obtained and fully characterised. The more active one was then immobilised on the metal–organic framework (MOF) solid support (Al)MIL-101-NH<sub>2</sub>. The catalytic activity of such a heterogeneous system was tested, showing that, while the heterogeneous catalyst is less active than the corresponding homogeneous catalyst in solution, it can catalyse selected olefin metathesis reactions, serving as the proof-of-concept for the immobilisation of catalytically active complexes in MOFs using a phenolic tag.

**Keywords:** olefin metathesis; ruthenium; metal–organic framework (MOF); immobilisation



**Citation:** Nadirova, M.; Cejas-Sánchez, J.; Sebastián, R.M.; Wiszniewski, M.; Chmielewski, M.J.; Kajetanowicz, A.; Grela, K. Synthesis of Phenol-Tagged Ruthenium Alkylidene Olefin Metathesis Catalysts for Robust Immobilisation Inside Metal–Organic Framework Support. *Catalysts* **2023**, *13*, 297. <https://doi.org/10.3390/catal13020297>

Academic Editors: Francis Verpoort and Somboon Chaemchuen

Received: 31 December 2022

Revised: 23 January 2023

Accepted: 25 January 2023

Published: 28 January 2023



**Copyright:** © 2023 by the authors. Licensee MDPI, Basel, Switzerland. This article is an open access article distributed under the terms and conditions of the Creative Commons Attribution (CC BY) license (<https://creativecommons.org/licenses/by/4.0/>).

## 1. Introduction

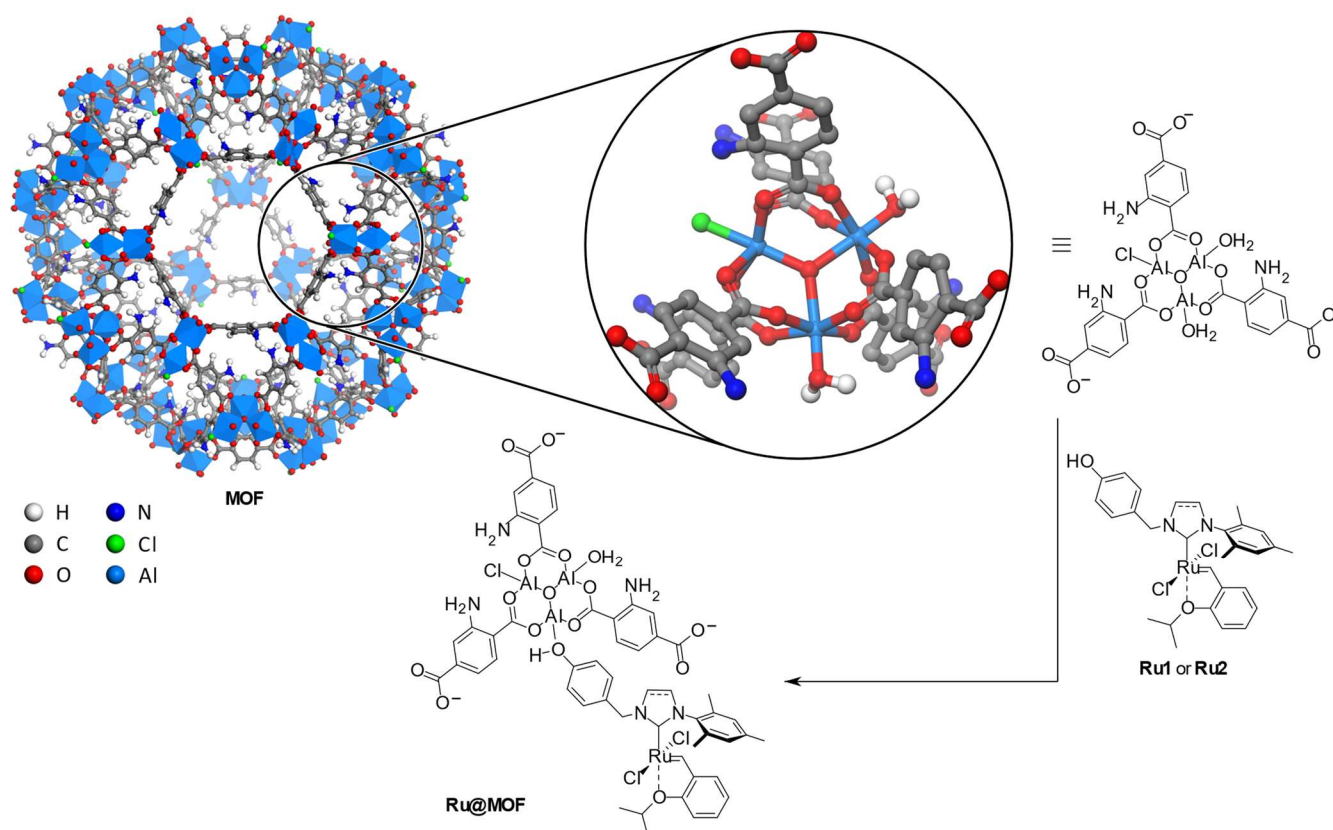
Olefin metathesis has emerged as one of the most powerful transformations in the tool cabinet of modern organic chemistry [1,2]. The rapid growth of its popularity is largely attributed to the discovery of stable, user-friendly ruthenium metathesis catalysts that combine high activity with good tolerance to air and moisture. Its high yield, atom-economic, selective nature, and ease of by-product (e.g., ethylene) separation has assisted its general acceptance in organic synthesis and process chemistry. On the other hand, metal complexes remaining after the olefin metathesis step may cause undesired side reactions such as product isomerisation, polymerisation, or degradation during work-up [3]. Therefore, the development of efficient and economical methods to remove ruthenium compounds present in the reaction mixture is crucial for the propagation of the metathesis methodology in industry. A number of efforts to remove the catalyst or the products of its decomposition by the addition of various scavengers such as peroxides, charcoal, silica gel, and other sorbents or by biphasic extraction have been carried out; however, none are universally applicable so far [3–5]. This situation has led to a tremendous interest in the supported or tagged versions of olefin metathesis catalysts.

One potentially very interesting class of supports is metal–organic frameworks (MOFs). MOFs are crystalline and porous coordination polymers, typically constructed from rigid organic ligands connected by metal ions or clusters (for a general introduction, see ref. [6], and for recent reviews on catalysis in MOFs, see refs. [7–10]). In contrast to some more conventional solid supports, such as activated carbons, amorphous silicas, and polymers, catalysts in MOFs are located inside well-defined nanoscopic voids in a highly porous crystalline framework. In this regard, MOFs resemble crystalline mesoporous silicas and zeolites, but surpass them by virtue of easy tunability, which they owe to their hybrid,

organic–inorganic nature. Indeed, by an appropriate choice of linkers and clusters, the voids in MOFs can be made large enough to encompass even the most intricate homogeneous catalysts and to allow free diffusion of substrates and products. Furthermore, cavities may be tailored for specific needs by appropriate functionalisation of the MOFs' organic ligands and/or coordination of functional moieties to the metal clusters. Therefore, catalysts immobilised in MOFs not only benefit from facile separation and potential reusability but are also site-separated from each other in a well-defined, tuneable nanoenvironment [8,11]. In the long term, the embedding framework may be envisaged to control substrate selectivity, regioselectivity, and even enantioselectivity of the immobilised catalysts, as well as confine different catalytic species for tandem or parallel catalysis.

However, robust immobilisation of active olefin metathesis catalysts inside MOFs is challenging. Such catalysts are unlikely to survive the typically harsh, solvothermal conditions of MOFs synthesis and, therefore, various strategies of their post-synthetic immobilisation have been developed. First, a small library of ammonium-tagged Ru-catalysts were non-covalently immobilised by Chmielewski et al. inside an aluminium-based MOF [12]. Quaternary ammonium cation-tagged ruthenium alkylidene complexes were supported inside (Al)MIL-101-NH<sub>2</sub>·HCl by simple impregnation, leading to solid heterogeneous catalysts stable even under continuous flow conditions. Structurally close Ru complexes featuring one or two ammonium tags were also immobilised via Coulomb interactions in the same (Al)MIL-101-NH<sub>2</sub>·HCl by Grela et al., who studied their mechanism of initiation and the propagation of Ru species during the catalytic cycle in this heterogeneous system [13]. Looking for more robust immobilisation methods, Chmielewski et al. used an acid–base neutralisation (a salt formation reaction) to immobilise Ru catalysts bearing basic nitrogen atoms (amine tags) on sulfonic acid-tagged MOFs [14]. In parallel, Kajtánowicz et al. studied the non-covalent immobilisation of a cationic ruthenium complex in a (Cr)MIL-101-SO<sub>3</sub>Na MOF by ion exchange (salt metathesis) [15]. In addition to the noncovalent immobilisation strategies described above, a mechanochemical procedure for the entrapment of a second-generation Hoveyda–Grubbs catalyst within the MOF was also elaborated [16]. Systems in which Ru catalysts were covalently bound to the MOF were disclosed by Yuan and Klemperer, who used an aldehyde-functionalised ruthenium catalyst to form an imine bond with an amine-functionalised IRMOF-74-III [17].

Unfortunately, none of the above-described strategies are universally applicable and free from disadvantages, so there is still a need to look for other modes of ruthenium olefin metathesis immobilisation in MOFs. In the present work, we have focused on using interaction between ruthenium catalysts featuring a phenolic tag and the coordinatively unsaturated sites in the aluminium-based MOF (Al)MIL-101-NH<sub>2</sub>. Despite the fact that the coordination of pyridines [18], aliphatic amines [19], carboxylates [20–23], and other donor moieties [24,25] with Lewis acidic centres in MOF clusters is well known and has already been utilised for the immobilisation of various catalytic species, to the best of our knowledge, phenols have never been utilised for this purpose (for a rare example of using phenol coordination to functionalise MOFs see ref. [26]). Because the more strongly basic donors such as amines and carboxylates are hardly compatible with olefin metathesis catalysts (and are likely to deactivate other transition metal catalysts, too), we envisaged that phenolic tags might serve as a viable alternative. Furthermore, upon coordination to the coordinatively unsaturated metal site, the phenolic OH becomes strongly acidic and is very likely to lose a proton, turning into a negatively charged ligand. Such a charge-assisted coordinate bond is clearly much stronger and might allow robust immobilisation. Therefore, we decided to check if phenol-tagged unsymmetrical-NHC-based Ru catalysts (for reviews on unsymmetrical-NHC-based Ru catalysts, see refs. [27,28]) can be immobilised inside a MOF, leading to the formation of stable heterogeneous catalysts (Scheme 1).

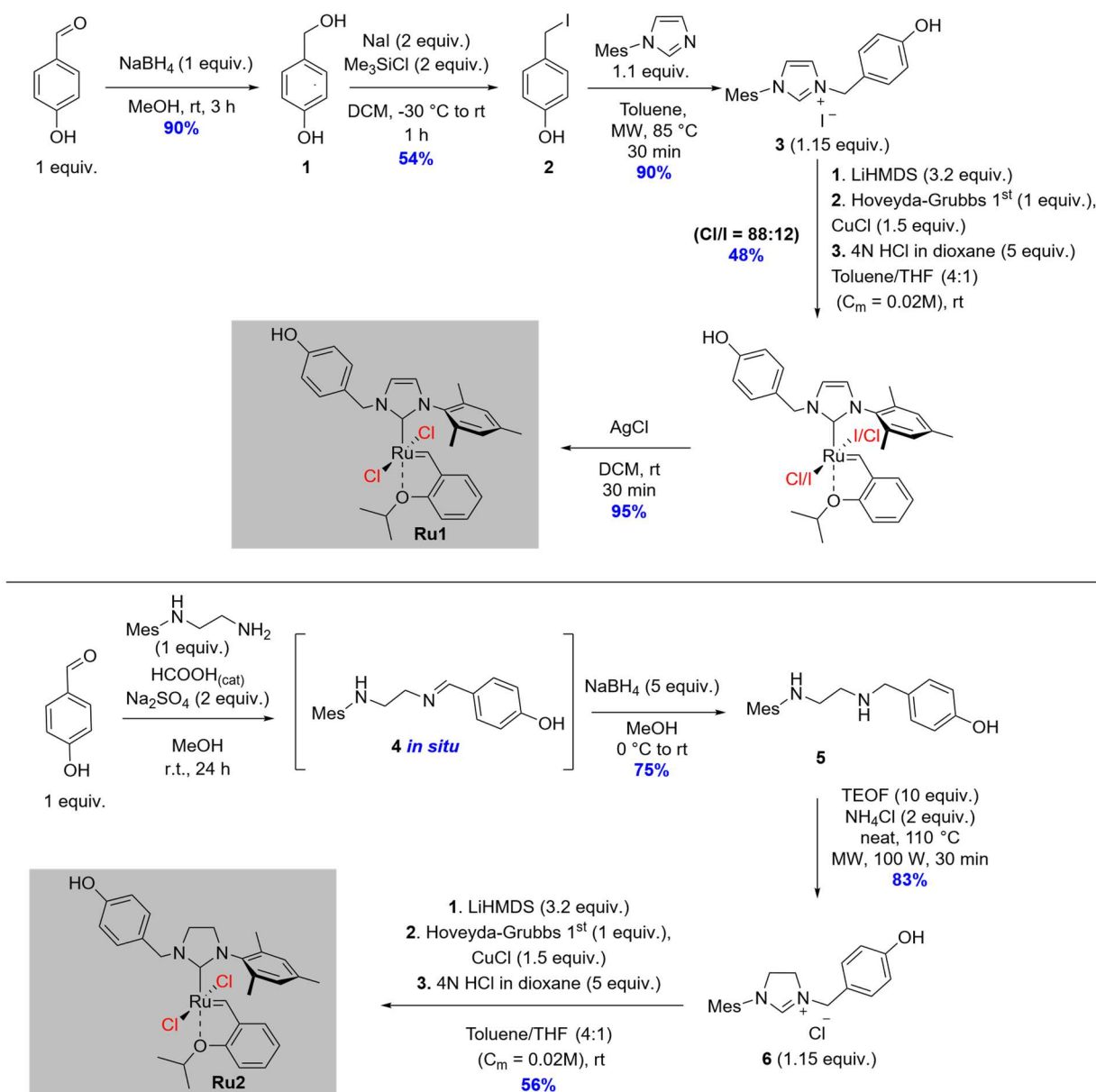


**Scheme 1.** Structure of (Al)MIL-101-NH<sub>2</sub> (hydrogen atoms were omitted for clarity) and the proposed mode of immobilisation of a phenol-tagged ruthenium complex.

## 2. Results and Discussion

**Synthesis of catalysts.** Synthesis of unsymmetrical imidazolium ligand precursors **3** and **6** was accomplished using two pathways: through simple alkylation of Mes (Mes = 2,4,6-trimethylphenyl)-bearing imidazole with 4-(iodomethyl)phenol (for **3**) or through condensation of *N*-(2,4,6-trimethylphenyl)-1,2-diaminoethane with 4-hydroxybenzaldehyde in the presence of a catalytic amount of formic acid (Scheme 2) [29]. The resulting imine **4** was reduced in situ to the corresponding diamine **5**, followed by cyclisation with triethyl orthoformate to give the NHC precursor **6**. The synthesis of uNHC Hoveyda–Grubbs-type II-generation complexes (uNHC = unsymmetrical NHC) was achieved via exchange of the phosphine ligand of the Hoveyda–Grubbs type I generation catalyst with an uNHC ligand. Treatment of a corresponding ligand precursor (**3** or **6**) with LiHMDS to generate a carbene in situ and reaction with the Hoveyda–Grubbs type I generation catalyst was followed by quenching with 5 equiv. of 4 N HCl in dioxane to “liberate” the OH-group provided the desired complexes **Ru1** and **Ru2** in moderate yields (Scheme 2). Interestingly, in the case of the **Ru1** complex, the exchange of Cl<sup>−</sup> anions at the ruthenium coordination centre to a labile iodide anion from the imidazolium ligand was observed. This so-called “scrambling” resulted in an undefined mixture of [Ru](Cl)<sub>2</sub> and [Ru](Cl/I)<sub>2</sub> complexes (see Supplementary Information, SI). To circumvent this obstacle, we decided to counter-exchange iodide anions to chlorides through treatment with silver chloride (1.1 equiv. *per* [Ru](Cl/I)<sub>2</sub> in DCM at room temperature) according to the previously reported method [30]. This simple transformation gave the pure **Ru1** complex in a practically quantitative yield (see SI).

The synthesised imidazolium ligand precursors (**3**, **6**) and catalysts (**Ru1**, **Ru2**) were fully characterised using the combination of NMR spectroscopy and HRMS (or elemental analysis), as well as IR spectroscopy. The chemical shifts of benzyldene protons of the obtained complexes ranged from 16.38 to 16.22 ppm, which is typical for this class of Hoveyda-type catalysts [31,32].



**Scheme 2.** Synthesis of unsymmetrical-NHC ligand precursors **3** and **6** and Ru catalysts **Ru1** and **Ru2** tagged with phenolic OH function.

**Stability studies.** Complexes **Ru1** and **Ru2** were dissolved in deuterated DCM ( $C_{[\text{Ru}]} = 0.02 \text{ M}$ ) in an argon atmosphere at room temperature, followed by the addition of 1,3,5-trimethoxybenzene as an internal standard. The decomposition of the catalysts was quantified using  $^1\text{H}$  NMR spectroscopy with respect to 1,3,5-trimethoxybenzene, by measuring the decrease in the intensity of benzylidene signals in  $^1\text{H}$  NMR spectra. Unfortunately, the analogous experiment performed in toluene failed due to precipitate formation. Both synthesised catalysts demonstrated high stability in deuterated DCM at room temperature, being decomposed in only 4% and 6% over 10 days (Figure 1). Comparing these results to what was reported previously for structurally related uNHC catalysts [31] shows a positive effect of the electron-donating OH-substituent in the *N*-benzyl “arm”, which visibly stabilised the ruthenium centre against decomposition.

**Catalytic performance preliminary studies.** Next, we decided to study the influence of the structural modification in the uNHC fragment on the activity of the newly obtained ruthenium complexes **Ru1** and **Ru2** bearing 4-hydroxybenzyl moiety in NHCs in olefin

metathesis. To do so, the ring-closing metathesis (RCM) reaction of diethyl diallyl malonate (DEDAM) (**7**) was evaluated as a model reaction. For this purpose, malonate **7** was dissolved in DCM or toluene ( $C_{[7]} = 0.1$  M) and treated with 1 mol% catalyst (**Ru1** or **Ru2**) [31,33]. The reaction was monitored through GC to determine the time-dependent conversion of **7**. As expected, similar to the other members of this uNHC catalysts family [29,31,34–38], both of the studied catalysts were found to be less active under ambient conditions, but sufficiently activated at slightly elevated temperature (Figure 2).

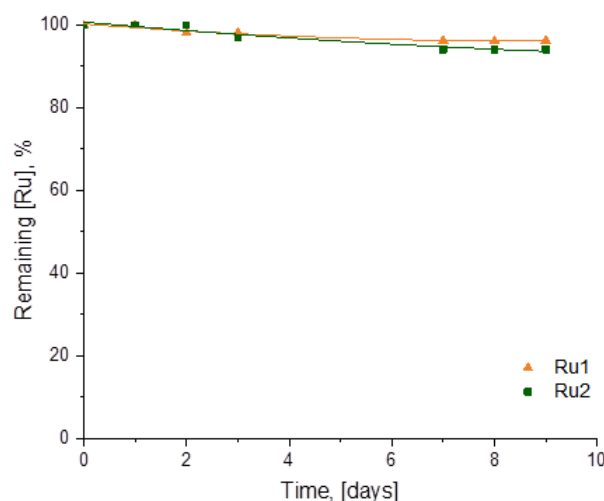


**Figure 1.** Results of the stability experiment for **Ru1** and **Ru2** in DCM- $d_2$  at room temperature.

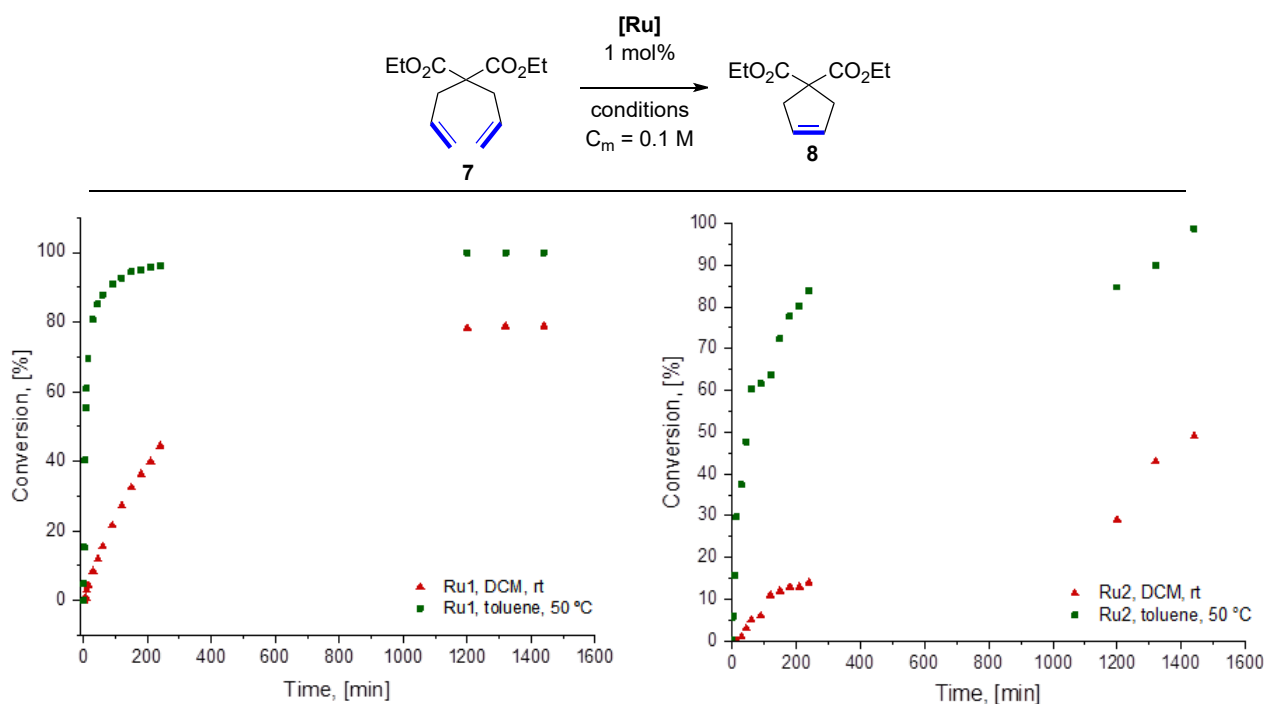


**Figure 2.** Time/conversion plot for the RCM reaction of **7** (0.1 M) catalysed by **Ru1** and **Ru2** (1 mol%) in DCM at 23 °C and in toluene at 50 °C. Conversion determined through GC.

In case of **Ru2**, the RCM experiment at room temperature in DCM showed a maximum conversion of 49%, demonstrating a rather moderate activity of the catalyst under ambient conditions. In the same manner, the RCM reaction of malonate **7** was also conducted using the unsaturated complex (**Ru1**). The outcome of this catalytic run was more positive—the conversion after 24 h reached 79%. When toluene was used as a solvent at 50 °C, both



catalysts showed satisfactory results, driving the reaction to full conversion. In this case, too, we could observe higher activity of **Ru1** compared to its saturated congener **Ru2**.

**Immobilisation of the ruthenium complex **Ru1** and desorption studies.** Next, we studied the sorption of the more active **Ru1** complex on a metal–organic framework (MOF). In search of an appropriate material, the relatively large size of the Hoveyda–Grubbs-type complexes and the stability of a potential solid support were taken into consideration. In this manner, we selected (Al)MIL-101-NH<sub>2</sub>, which met the aforementioned criteria [39]. Thus, the catalyst **Ru1** (approximately 10 w/w%) was dissolved in DCM or toluene (1 mM) followed by the addition of an appropriate amount of (Al)MIL-101-NH<sub>2</sub> (see SI). After 1 h of stirring, the mixture was centrifuged and the supernatant was examined using spectrophotometric methods, determining the catalyst concentration in the supernatant [12]. As a result, in both DCM and toluene, an *almost quantitative sorption* was observed (Table 1, 99.2% and 99.4% of the catalyst was absorbed in (Al)MIL-101-NH<sub>2</sub>, respectively). Since the catalyst was held inside the MOF by reversible noncovalent interactions, the desorption was the next in line to investigate. Therefore, we investigated the robustness of the catalyst's immobilisation by washing the obtained **Ru1@AlMIL-101-NH<sub>2</sub>** with toluene and DCM, starting with the less polar toluene. To do so, we placed the material on a G4 filtering funnel with side argon inlet (see Supplementary Material for a photo) and slowly filtered the solvents through the **catalyst@MOF**. The supernatants were monitored using UV-Vis. Interestingly, we did not observe any significant leaching of the absorbed catalyst from (Al)MIL-101-NH<sub>2</sub> under these challenging dynamic conditions—the total amount of **Ru1** washed out with toluene (20 mL) and DCM (20 mL) was less than 10% (Figure 3).

**Table 1.** Results of absorption experiments of **Ru1** from toluene and DCM.

Catalyst/Solvent	The Amount of Catalyst Adsorbed from Solution [%]
<b>Ru1</b> /Toluene	99.4
<b>Ru1</b> /DCM	99.2

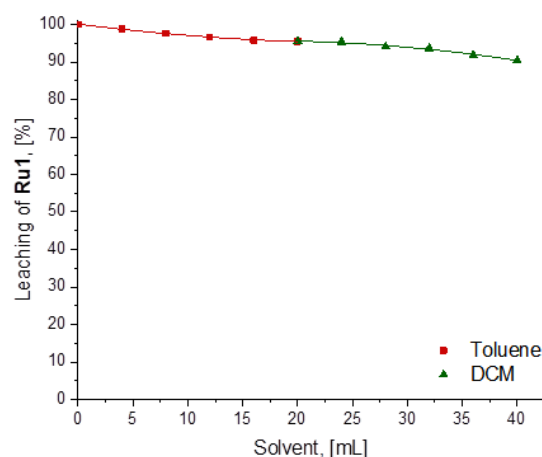


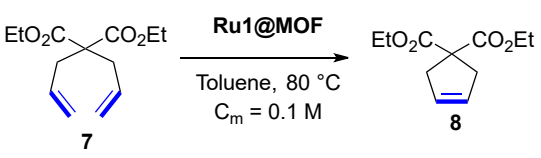
**Figure 3.** Desorption of **Ru1** catalyst from (Al)MIL-101-NH<sub>2</sub> by subsequent washing with toluene and later with DCM.

Powder X-ray diffraction (PXRD) studies revealed that the material remained crystalline after catalyst immobilisation, but its porosity, expressed as BET surface area, dropped significantly from 1753 m<sup>2</sup>/g for pristine MOF to 564 m<sup>2</sup>/g for **Ru1@AlMIL-101-NH<sub>2</sub>**.

**Catalytic studies.** The catalytic activity of the newly obtained **Ru1@AlMIL-101-NH<sub>2</sub>** material was investigated in the model ring-closing metathesis reaction of **7** in toluene at 80 °C with 1 mol% of the heterogenised catalyst (see Table 2). Based on the leaching experiment, the less polar medium leads to the negligible desorption from the solid support and, therefore, the choice of toluene as a solvent was more favourable in this case.

Compared to the homogeneous catalysis discussed earlier (Figure 2) where the conversion was quantitative, the heterogenised system **Ru1@(Al)MIL-101-NH<sub>2</sub>** demonstrated a poorer performance. After 24 h of reaction, only 54% of conversion was achieved under these conditions. As a matter of fact, increasing the **Ru1@(Al)MIL-101-NH<sub>2</sub>** loading up to 2 mol% did not lead to increased conversion.

**Table 2.** Results of the RCM reaction of DEDAM (**7**) with **Ru1** and **Ru1@(Al)MIL-101-NH<sub>2</sub>** complexes in toluene. ( $C_{[7]} = 0.1$  M). Conversion was determined through GC (tetradecane was used as an internal standard).

		
[Ru]	Time, [h]	Conversion, [%]
<b>Ru1</b> (1 mol%) homogeneous	3	95
	24	>99
<b>Ru1@MOF</b> (1 mol%) heterogeneous	3	53
	24	54
<b>Ru1@MOF</b> (2 mol%) heterogeneous	3	50
	24	51

Next, we decided to test the new system on a set of olefin metathesis substrates with the standard loading (1 mol%) of **Ru1@MOF**. Surprisingly, excellent results were obtained in the RCM reaction of DATA (**11**)—the conversion reached 65% in 3 h and 91% in 24 h. It should be mentioned here that we tried to improve the catalyst performance by treating the MOF with dry HCl in Et<sub>2</sub>O after sorption of the catalyst [12]. Interestingly, the conversion of DATA (**11**) in the reaction catalysed with **Ru1@(Al)MIL-101-NH<sub>2</sub>·HCl** reached 78% in just 15 min, but, unfortunately, did not increase after 24 h. Disappointingly, the RCM reaction of the olefin metathesis substrates **9** and **13** conducted in a similar manner (1 mol% of **Ru1@(Al)MIL-101-NH<sub>2</sub>**) resulted in a poorer outcome, giving only 31 and 30% conversion, respectively (see Table 3).

**Table 3.** Results of the RCM reaction of selected dienes catalysed by **Ru1@(Al)MIL-101-NH<sub>2</sub>** complex in toluene at 80 °C. ( $C_{[7]} = 0.1$  M). Conversion was determined through GC (tetradecane was used as an internal standard).

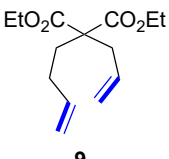
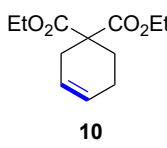
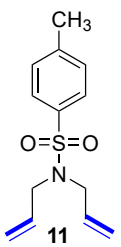
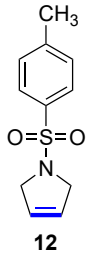
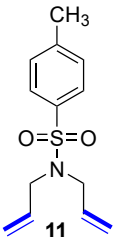
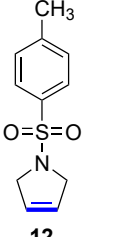
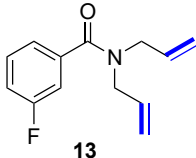
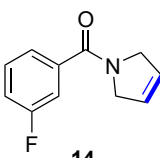
[Ru]@MOF	Substrate	Product	Conversion in 24 h
<b>Ru1@(Al)MIL-101-NH<sub>2</sub></b>	 <b>9</b>	 <b>10</b>	31
	 <b>11</b>	 <b>12</b>	91

Table 3. Cont.

[Ru]@MOF	Substrate	Product	Conversion in 24 h
Ru1@(Al)MIL-101-NH <sub>2</sub> ·HCl	 11	 12	78
Ru1@(Al)MIL-101-NH <sub>2</sub>	 13	 14	30

### 3. Materials and Methods

**General Remarks.** All reactions requiring exclusion of oxygen and moisture were carried out in dry glassware with dry solvents (SPS MBraun) under a dry and oxygen-free argon atmosphere using the standard Schlenk technique. The addition of dry solvents or reagents was carried out using argon-flushed plastic syringes.

Analytical thin layer chromatography (TLC) was performed on Merck Silica gel 60 F254 precoated aluminium sheets. Components were visualised by observation under UV light (254 nm or 365 nm) or dyed using aqueous KMnO<sub>4</sub> or anisaldehyde reagent. Flash column chromatography was carried out using silica gel 60 (230–400 mesh), purchased from Merck. GC chromatograms were recorded using a PerkinElmer Clarus 580 model. As the capillary column, an IntertCap 5MS-Sil column was employed with helium as the carrier gas. GC conversions were determined based on the ratio of an internal standard (trimethoxybenzene or tetradecane) and the starting material. <sup>1</sup>H NMR spectra were recorded in DCM-*d*<sub>2</sub>, DMSO-*d*<sub>6</sub>, and MeOH-*d*<sub>4</sub> at room temperature on Agilent Mercury spectrometers (400 MHz). The data were interpreted in first-order spectra. Chemical shifts  $\delta$  are reported in parts per million (ppm) downfield from trimethylsilane as reference to residual solvent signal: DCM-*d*<sub>2</sub> [ $\delta$ H = 5.32 ppm], DMSO-*d*<sub>6</sub> [ $\delta$ H = 2.50 ppm], D<sub>2</sub>O [ $\delta$ H = 4.79 ppm], and MeOH-*d*<sub>4</sub> [ $\delta$ H = 3.31 ppm]. The following abbreviations are used to indicate the signal multiplicity: s (singlet), d (doublet), t (triplet), q (quartet), quin (quintet), sext (sextet), dd (doublet of doublet), dt (doublet of triplet), ddd (doublet of doublet of doublet), etc., br. s (broad signal), and m (multiplet). Coupling constants (*J*) are given in Hz and refer to H,H-couplings. <sup>13</sup>C NMR spectra were recorded at room temperature on Agilent Mercury 101 MHz spectrometers. The spectra were recorded in DCM-*d*<sub>2</sub>, DMSO-*d*<sub>6</sub>, and MeOH-*d*<sub>4</sub>. Chemical shifts are reported in  $\delta$  units relative to the solvent signal: DCM-*d*<sub>2</sub> [ $\delta$ C = 53.84 ppm], DMSO-*d*<sub>6</sub> [ $\delta$ C = 39.52 ppm], and MeOH-*d*<sub>4</sub> [ $\delta$ C = 49.00 ppm]. High resolution mass spectra (HR-MS) were obtained on an AutoSpec Premier spectrometer. Elemental analyses were carried out at the Polish Academy of Science, Institute of Organic Chemistry. IR spectra were recorded on a Perkin-Elmer Spectrum One FTIR spectrometer. Substances were applied as a film, solid, or in solution. The obtained data were processed with the software Omni32. Wavenumbers are given in cm<sup>−1</sup>. Powder X-ray diffraction: All powder X-ray diffraction (PXRD) patterns were recorded on a Bruker D8 Discover X-ray diffractometer (CuK $\alpha$  radiation), with a parallel beam formed by a Goebel mirror equipped with a VANTEC 1 position-sensitive detector. All measurements were performed in an aluminium holder. The nitrogen adsorption isotherms were measured at liquid nitrogen temperature (77 K) using Quantachrome Autosorb-IQ-MP sorption analyser. Prior to



measurements, all samples were dried for no less than 24 h under vacuum ( $2 \times 10^{-2}$  mbar) at room temperature. The specific surface areas were calculated according to the Brunauer-Emmett-Teller (BET) method. For all isotherm analyses we ensured that the two consistency criteria described by Rouquerol et al. [40] and Walton et al. [41] were satisfied.

**Reagents and Solvents:** All reagents were purchased from Sigma-Aldrich, Apeiron Synthesis, and POCH and used without further purification unless stated otherwise.

**General Procedure for Synthesis of Ru Complexes:** In a dried 50 mL Schleck flask, the corresponding NHC ligand **3** or **6** (1.15 equiv.) was suspended in dry toluene (12 mL). To the resulting suspension, LiHDMS (3.2 equiv.) was added, and the mixture was stirred for 1 h at room temperature in an atmosphere of argon. To this suspension, 3 mL of dry THF was added and the reaction was stirred until the solution became clear and homogeneous. To this clear solution, Hoveyda–Grubbs type I generation (**Hov I**) was added (124 mg, 0.206 mmol, 1.0 equiv.). The resulting solution was stirred at room temperature for 2 h (the reaction was monitored by TLC, 50% AcOEt/*n*-hexane). After the complete disappearance of **Hov I** on TLC, CuCl (31 mg, 0.31 mmol, 1.5 equiv.) was added to the reaction and it was stirred for an additional 30 min, followed by the dropwise addition of 4N HCl in dioxane (0.258 mL). The reaction mixture was stirred for another 30 min, transferred to a round bottom flask, and volatiles were evaporated to dryness. The crude mixture was purified through column chromatography (20% to 50% AcOEt/*n*-hexane).

**Synthesis of Ruthenium Complex Ru1:** Ruthenium complex **Ru1** was synthesised following the general procedure, using NHC ligand **3** (100 mg, 0.238 mmol, 1.15 equiv.), LiHDMS (110 mg, 0.66 mmol, 3.2 equiv.), **Hov I** (124 mg, 0.206 mmol, 1.0 equiv.), CuCl (31 mg, 0.31 mmol, 1.5 equiv.) and 4N HCl in dioxane (0.258 mL, 1.03 mmol). The desired product was crystallised from the mixture of DCM/MeOH (3:1) to give a fine dark-green powder (60 mg, 0.1 mmol, 48%). The ratio of Cl/I at the ruthenium coordination centre was established based on integration of benzyldiene signals by  $^1\text{H}$  NMR as 88:12. An oven-dried vial was charged with AgCl (1.1 equiv. per iodide) and Ru-complex (30 mg). The vial was evacuated and flushed with argon three times, dry DCM (1 mL) was added, and the resulting mixture was stirred for 30 min at room temperature. The resulting solution was centrifuged, filtered through a Celite<sup>®</sup> pad, and washed with MeOH (20 mL). Solvents were evaporated and the residue was crystallised from the mixture of DCM/MeOH and dried under vacuum overnight to provide a pure product as a fine dark-green powder (90%).  $^1\text{H}$  NMR (400 MHz,  $\text{CD}_2\text{Cl}_2$ )  $\delta$  16.38 (s, 1H), 7.60 (ddd,  $J = 8.4, 7.2, 1.9$  Hz, 1H), 7.54 (d,  $J = 8.5$  Hz, 2H), 7.17 (m, 2H), 7.11–6.98 (m, 3H), 6.93 (dd,  $J = 5.4, 3.2$  Hz, 3H), 6.87 (d,  $J = 2.1$  Hz, 1H), 6.08 (s, 2H), 5.45 (s, 1H), 5.21 (hept,  $J = 6.2$  Hz, 1H), 2.53 (s, 3H), 2.04 (d,  $J = 0.7$  Hz, 6H), 1.76 (d,  $J = 6.1$  Hz, 6H).  $^{13}\text{C}$  NMR (101 MHz,  $\text{CD}_2\text{Cl}_2$ )  $\delta$  287.5, 172.3, 156.2, 152.4, 144.1, 139.8, 137.2, 131.1, 129.1, 129.0, 127.9, 124.4, 122.6, 121.7, 121.2, 115.6, 112.9, 75.3, 54.8, 21.8, 21.0, 17.6. EA: calculated for  $\text{C}_{29}\text{H}_{32}\text{Cl}_2\text{N}_2\text{O}_2\text{Ru}$ : C, 56.86; H, 5.27; N, 4.57; Found C, 56.59; H, 5.48; N, 4.34.

**Synthesis of Ruthenium Complex Ru2:** Ruthenium complex **Ru2** was synthesised following the general procedure, using NHC ligand **6** (100 mg, 0.3 mmol, 1.15 equiv.), LiHDMS (110 mg, 0.66 mmol, 3.2 equiv.), **Hov I** (158 mg, 0.263 mmol, 1.0 equiv.), CuCl (39.4 mg, 0.39 mmol, 1.5 equiv.) and 4N HCl in dioxane (0.118 mL, 1.31 mmol). The desired product was crystallised from the mixture of DCM/MeOH (3:1) to give a fine dark-green powder (72 mg, 0.12 mmol, 56%).  $^1\text{H}$  NMR (400 MHz,  $\text{CD}_2\text{Cl}_2$ )  $\delta$  16.22 (s, 1H), 7.67–7.54 (m, 3H), 7.11 (s, 2H), 7.04–6.95 (m, 3H), 6.90 (d,  $J = 7.8$  Hz, 2H), 5.53 (s, 2H), 5.18 (hept,  $J = 6.1$  Hz, 1H), 3.92 (t,  $J = 10.0$  Hz, 2H), 3.64 (d,  $J = 10.0$  Hz, 2H), 2.48 (s, 3H), 2.24 (s, 6H), 2.01 (s, 1H), 1.71 (d,  $J = 6.1$  Hz, 6H).  $^{13}\text{C}$  NMR (101 MHz,  $\text{CD}_2\text{Cl}_2$ )  $\delta$  152.2, 138.9, 138.0, 137.7, 130.6, 129.5, 129.5, 122.5, 122.1, 115.3, 112.86, 75.2, 47.7, 21.8, 20.9, 17.7.

#### 4. Conclusions

Two new uNHC-based ruthenium complexes featuring phenolic OH function were obtained and fully characterised. The more active one was then successfully immobilised on the MOF support. Desorption studies suggest that the highly porous structure of

(Al)MIL-101-NH<sub>2</sub> offers a favourable environment for the non-covalent immobilisation of a phenol-tagged ruthenium catalyst. After immobilisation, the Lewis acidic coordinatively unsaturated centres located inside the well-defined nanoscopic voids in a crystalline framework of the MOF strongly bind the ruthenium complex, which results in negligible leaching even in polar solvent, such as DCM. The catalytic activity of such a formed heterogeneous system was unfortunately lower than the activity of the corresponding homogeneous catalyst in solution; however, it was found to catalyse selected olefin metathesis reactions. We believe that the results reported herein create a valid proof-of-concept and are the very first example of catalyst immobilisation by means of phenol–MOF interaction.

**Supplementary Materials:** The following supporting information can be downloaded at: <https://www.mdpi.com/article/10.3390/catal13020297/s1>. Figure S1. <sup>1</sup>H NMR spectrum of (Al)MIL-101-NH<sub>2</sub> digested in 4 wt. % NaOD/D<sub>2</sub>O; Figure S2. Powder X-ray diffraction (PXRD) pattern of (Al)MIL-101-NH<sub>2</sub>; Figure S3. N<sub>2</sub> adsorption/desorption isotherm of (Al)MIL-101-NH<sub>2</sub>. Points in the range  $p/p_0 = 0.0005$ – $0.21$  were used to calculate BET surface area; Figure S4. UV-Vis spectra of catalysts **Ru1** and **Ru2** and determination of their molar absorption coefficients  $\epsilon$ ; Figure S5. Powder X-ray diffraction (PXRD) pattern of **Ru1@ (Al)MIL-101-NH<sub>2</sub>**; Figure S6. N<sub>2</sub> adsorption/desorption of **Ru1@ (Al)MIL-101-NH<sub>2</sub>**. Points in the range  $p/p_0 = 0.0005$ – $0.21$  were used to calculate BET surface area; Figure S7. Glassware used in the desorption (leaching) experiments; Figure S8. <sup>1</sup>H NMR of compound **1**; Figure S9. <sup>13</sup>C NMR of compound **1**; Figure S10. <sup>1</sup>H NMR of compound **3**; Figure S11. <sup>13</sup>C NMR of compound **3**; Figure S12. <sup>1</sup>H NMR of compound **5**; Figure S13. <sup>13</sup>C NMR of compound **5**; Figure S14. <sup>1</sup>H NMR of compound **6**; Figure S15. <sup>13</sup>C NMR of compound **6**; Figure S16. <sup>1</sup>H NMR of **Ru1** after the crystallization from DCM/MeOH; Figure S17. <sup>1</sup>H NMR of **Ru1** after stirring it with AgCl; Figure S18. <sup>13</sup>C NMR of **Ru1** after stirring it with AgCl; Figure S19. <sup>1</sup>H NMR of **Ru2**; Figure S20. <sup>13</sup>C NMR of **Ru2**; Figure S21. <sup>1</sup>H NMR of compound **15**; Figure S22. <sup>13</sup>C NMR of compound **15**; Table S1. Stability studies of **Ru1** and **Ru2** in CD<sub>2</sub>Cl<sub>2</sub>; Table S2. Conditions of the RCM reaction and conversion of diethyl diallylmalonate (**7**) in the presence of 1 mol% **Ru1** or **Ru2**; Table S3. Results of absorption experiments of **Ru1** in DCM and toluene [42,43].

**Author Contributions:** Conceptualization, M.J.C. and K.G.; methodology, M.J.C.; investigation, M.N., J.C.-S. and M.W.; resources, M.J.C.; writing—original draft, M.N., M.J.C. and K.G.; writing—review & editing, M.N., J.C.-S., M.W., R.M.S., M.J.C., A.K. and K.G.; Visualization, M.W. and K.G.; Supervision, M.J.C., A.K. and K.G.; Funding acquisition, M.J.C. and K.G. All authors have read and agreed to the published version of the manuscript.

**Funding:** This research received funding from: European Union’s Horizon 2020 research and innovation programme (Marie Skłodowska-Curie grant agreement No 860322) and National Science Centre, Poland (OPUS grant 2017/27/B/ST5/00941).

**Data Availability Statement:** Data supporting reported results of this study are available in the supplementary material of this article and can be obtained from the corresponding author.

**Acknowledgments:** This work was supported by the European Union’s Horizon 2020 research and innovation programme under the Marie Skłodowska-Curie grant agreement No 860322 for the ITN-EJD “Coordination Chemistry Inspires Molecular Catalysis” (CCIMC). MJC and MW thank the National Science Centre, Poland (OPUS grant 2017/27/B/ST5/00941), for funding.

**Conflicts of Interest:** The authors declare no conflict of interest.

## References

1. Grela, K. (Ed.) *Olefin Metathesis: Theory and Practice*; John Wiley & Sons, Inc.: Hoboken, NJ, USA, 2014.
2. Grubbs, R.H.; Wenzel, A.G.; O’Leary, D.J.; Khosravi, E. (Eds.) *Handbook of Metathesis*; Wiley-VCH: Weinheim, Germany, 2015.
3. Clavier, H.; Grela, K.; Kirschning, A.; Mauduit, M.; Nolan, S.P. Sustainable Concepts in Olefin Metathesis. *Angew. Chem. Int. Ed.* **2007**, *46*, 6786–6801. [CrossRef] [PubMed]
4. Vougioukalakis, G.C. Removing Ruthenium Residues from Olefin Metathesis Reaction Products. *Chem.—A Eur. J.* **2012**, *18*, 8868–8880. [CrossRef] [PubMed]
5. Wheeler, P.; Phillips, J.H.; Pederson, R.L. Scalable Methods for the Removal of Ruthenium Impurities from Metathesis Reaction Mixtures. *Org. Process Res. Dev.* **2016**, *20*, 1182–1190. [CrossRef]

6. Yaghi, O.M.; Kalmutzki, M.J.; Diercks, C.S. (Eds.) *Introduction to Reticular Chemistry: Metal–Organic Frameworks and Covalent Organic Frameworks*; Wiley-VCH: Weinheim, Germany, 2019.
7. Dybtsev, D.N.; Bryliakov, K.P. Asymmetric catalysis using metal–organic frameworks. *Coord. Chem. Rev.* **2021**, *437*, 213845. [[CrossRef](#)]
8. Wei, Y.-S.; Zhang, M.; Zou, R.; Xu, Q. Metal–Organic Framework-Based Catalysts with Single Metal Sites. *Chem. Rev.* **2020**, *120*, 12089–12174. [[CrossRef](#)]
9. Bavykina, A.; Kolobov, N.; Khan, I.S.; Bau, J.A.; Ramirez, A.; Gascon, J. Metal–Organic Frameworks in Heterogeneous Catalysis: Recent Progress, New Trends, and Future Perspectives. *Chem. Rev.* **2020**, *120*, 8468–8535. [[CrossRef](#)]
10. Yang, D.; Gates, B.C. Catalysis by Metal Organic Frameworks: Perspective and Suggestions for Future Research. *ACS Catal.* **2019**, *9*, 1779–1798. [[CrossRef](#)]
11. Rogge, S.M.J.; Bavykina, A.; Hajek, J.; Garcia, H.; Olivos-Suarez, A.I.; Sepúlveda-Escribano, A.; Vimont, A.; Clet, G.; Bazin, P.; Kapteijn, F.; et al. Metal–organic and covalent organic frameworks as single-site catalysts. *Chem. Soc. Rev.* **2017**, *46*, 3134–3184. [[CrossRef](#)]
12. Chołuj, A.; Zieliński, A.; Grela, K.; Chmielewski, M.J. Metathesis@MOF: Simple and Robust Immobilization of Olefin Metathesis Catalysts inside (Al)MIL-101-NH<sub>2</sub>. *ACS Catal.* **2016**, *6*, 6343–6349. [[CrossRef](#)]
13. Chołuj, A.; Nogaś, W.; Patrzalek, M.; Krzesiński, P.; Chmielewski, M.J.; Kajetanowicz, A.; Grela, K. Preparation of Ruthenium Olefin Metathesis Catalysts Immobilized on MOF, SBA-15, and 13X for Probing Heterogeneous Boomerang Effect. *Catalysts* **2020**, *10*, 438. [[CrossRef](#)]
14. Chołuj, A.; Karczykowski, R.; Chmielewski, M.J. Simple and Robust Immobilization of a Ruthenium Olefin Metathesis Catalyst Inside MOFs by Acid–Base Reaction. *Organometallics* **2019**, *38*, 3392–3396. [[CrossRef](#)]
15. Chołuj, A.; Krzesiński, P.; Ruszczyńska, A.; Bulska, E.; Kajetanowicz, A.; Grela, K. Noncovalent Immobilization of Cationic Ruthenium Complex in a Metal–Organic Framework by Ion Exchange Leading to a Heterogeneous Olefin Metathesis Catalyst for Use in Green Solvents. *Organometallics* **2019**, *38*, 3397–3405. [[CrossRef](#)]
16. Spekrijse, J.; Öhrström, L.; Sanders, J.P.M.; Bitter, J.H.; Scott, E.L. Mechanochemical Immobilisation of Metathesis Catalysts in a Metal–Organic Framework. *Chem.—A Eur. J.* **2016**, *22*, 15437–15443. [[CrossRef](#)]
17. Yuan, J.; Fracaroli, A.M.; Klemperer, W.G. Convergent Synthesis of a Metal–Organic Framework Supported Olefin Metathesis Catalyst. *Organometallics* **2016**, *35*, 2149–2155. [[CrossRef](#)]
18. Arnanz, A.; Pintado-Sierra, M.; Corma, A.; Iglesias, M.; Sánchez, F. Bifunctional Metal Organic Framework Catalysts for Multistep Reactions: MOF-Cu(BTC)-[Pd] Catalyst for One-Pot Heteroannulation of Acetylenic Compounds. *Adv. Synth. Catal.* **2012**, *354*, 1347–1355. [[CrossRef](#)]
19. Sivan, S.E.; Oh, K.-R.; Yoon, J.-W.; Yoo, C.; Hwang, Y.K. Immobilization of a trimeric ruthenium cluster in mesoporous chromium terephthalate and its catalytic application. *Dalton Trans.* **2022**, *51*, 13189–13194. [[CrossRef](#)] [[PubMed](#)]
20. Berijani, K.; Morsali, A.; Hupp, J.T. An effective strategy for creating asymmetric MOFs for chirality induction: A chiral Zr-based MOF for enantioselective epoxidation. *Catal. Sci. Technol.* **2019**, *9*, 3388–3397. [[CrossRef](#)]
21. Rimoldi, M.; Nakamura, A.; Vermeulen, N.A.; Henkelis, J.J.; Blackburn, A.K.; Hupp, J.T.; Stoddart, J.F.; Farha, O.K. A metal–organic framework immobilised iridium pincer complex. *Chem. Sci.* **2016**, *7*, 4980–4984. [[CrossRef](#)]
22. Baek, J.; Rungtaweeworanit, B.; Pei, X.; Park, M.; Fakra, S.C.; Liu, Y.-S.; Matheu, R.; Alshimri, S.A.; Alshehri, S.; Trickett, C.A.; et al. Bioinspired Metal–Organic Framework Catalysts for Selective Methane Oxidation to Methanol. *J. Am. Chem. Soc.* **2018**, *140*, 18208–18216. [[CrossRef](#)]
23. Choi, S.; Jung, W.-J.; Park, K.; Kim, S.-Y.; Baeg, J.-O.; Kim, C.H.; Son, H.-J.; Pac, C.; Kang, S.O. Rapid Exciton Migration and Amplified Funneling Effects of Multi-Porphyrin Arrays in a Re(I)/Porphyrinic MOF Hybrid for Photocatalytic CO<sub>2</sub> Reduction. *ACS Appl. Mater. Interfaces* **2021**, *13*, 2710–2722. [[CrossRef](#)]
24. Wu, P.; He, C.; Wang, J.; Peng, X.; Li, X.; An, Y.; Duan, C. Photoactive Chiral Metal–Organic Frameworks for Light-Driven Asymmetric  $\alpha$ -Alkylation of Aldehydes. *J. Am. Chem. Soc.* **2012**, *134*, 14991–14999. [[CrossRef](#)] [[PubMed](#)]
25. Madrahimov, S.T.; Gallagher, J.R.; Zhang, G.; Meinhart, Z.; Garibay, S.J.; Delferro, M.; Miller, J.T.; Farha, O.K.; Hupp, J.T.; Nguyen, S.T. Gas-Phase Dimerization of Ethylene under Mild Conditions Catalyzed by MOF Materials Containing (bpy)NiII Complexes. *ACS Catal.* **2015**, *5*, 6713–6718. [[CrossRef](#)]
26. Zhu, W.; Xiang, G.; Shang, J.; Guo, J.; Motevalli, B.; Durfee, P.; Agola, J.O.; Coker, E.N.; Brinker, C.J. Versatile Surface Functionalization of Metal–Organic Frameworks through Direct Metal Coordination with a Phenolic Lipid Enables Diverse Applications. *Adv. Funct. Mater.* **2018**, *28*, 1705274. [[CrossRef](#)]
27. Monsigny, L.; Kajetanowicz, A.; Grela, K. Ruthenium Complexes Featuring Unsymmetrical N-Heterocyclic Carbene Ligands—Useful Olefin Metathesis Catalysts for Special Tasks. *Chem. Rec.* **2021**, *21*, 3648–3661. [[CrossRef](#)] [[PubMed](#)]
28. Paradiso, V.; Costabile, C.; Grisi, F. Ruthenium-based olefin metathesis catalysts with monodentate unsymmetrical NHC ligands. *Beilstein J. Org. Chem.* **2018**, *14*, 3122–3149. [[CrossRef](#)]
29. Abilalimov, O.; Kędziorek, M.; Torborg, C.; Malińska, M.; Woźniak, K.; Grela, K. New Ruthenium(II) Indenylidene Complexes Bearing Unsymmetrical N-Heterocyclic Carbenes. *Organometallics* **2012**, *31*, 7316–7319. [[CrossRef](#)]
30. Patrzalek, M.; Piątkowski, J.; Kajetanowicz, A.; Grela, K. Anion Metathesis in Facile Preparation of Olefin Metathesis Catalysts Bearing a Quaternary Ammonium Chloride Tag. *Synlett* **2019**, *30*, 1981–1987. [[CrossRef](#)]

31. Małecki, P.; Gajda, K.; Ablialimov, O.; Malińska, M.; Gajda, R.; Woźniak, K.; Kajetanowicz, A.; Grela, K. Hoveyda–Grubbs-Type Precatalysts with Unsymmetrical N-Heterocyclic Carbenes as Effective Catalysts in Olefin Metathesis. *Organometallics* **2017**, *36*, 2153–2166. [\[CrossRef\]](#)
32. Małecki, P.; Gajda, K.; Gajda, R.; Woźniak, K.; Trzaskowski, B.; Kajetanowicz, A.; Grela, K. Specialized Ruthenium Olefin Metathesis Catalysts Bearing Bulky Unsymmetrical NHC Ligands: Computations, Synthesis, and Application. *ACS Catal.* **2019**, *9*, 587–598. [\[CrossRef\]](#)
33. Planer, S.; Małecki, P.; Trzaskowski, B.; Kajetanowicz, A.; Grela, K. Sterically Tuned N-Heterocyclic Carbene Ligands for the Efficient Formation of Hindered Products in Ru-Catalyzed Olefin Metathesis. *ACS Catal.* **2020**, *10*, 11394–11404. [\[CrossRef\]](#)
34. Smoleń, M.; Kośnik, W.; Loska, R.; Gajda, R.; Malińska, M.; Woźniak, K.; Grela, K. Synthesis and catalytic activity of ruthenium indenylidene complexes bearing unsymmetrical NHC containing a heteroaromatic moiety. *RSC Adv.* **2016**, *6*, 77013–77019. [\[CrossRef\]](#)
35. Grudzień, K.; Trzaskowski, B.; Smoleń, M.; Gajda, R.; Woźniak, K.; Grela, K. Hoveyda–Grubbs catalyst analogues bearing the derivatives of N-phenylpyrrol in the carbene ligand-structure, stability, activity and unique ruthenium-phenyl interactions. *Dalton Trans.* **2017**, *46*, 11790–11799. [\[CrossRef\]](#) [\[PubMed\]](#)
36. Smoleń, M.; Kośnik, W.; Gajda, R.; Woźniak, K.; Skoczeń, A.; Kajetanowicz, A.; Grela, K. Ruthenium Complexes Bearing Thiophene-Based Unsymmetrical N-Heterocyclic Carbene Ligands as Selective Catalysts for Olefin Metathesis in Toluene and Environmentally Friendly 2-Methyltetrahydrofuran. *Chem.—A Eur. J.* **2018**, *24*, 15372–15379. [\[CrossRef\]](#) [\[PubMed\]](#)
37. Ablialimov, O.; Kędziorek, M.; Malińska, M.; Woźniak, K.; Grela, K. Synthesis, Structure, and Catalytic Activity of New Ruthenium(II) Indenylidene Complexes Bearing Unsymmetrical N-Heterocyclic Carbenes. *Organometallics* **2014**, *33*, 2160–2171. [\[CrossRef\]](#)
38. Jolly, P.I.; Marczyk, A.; Małecki, P.; Ablialimov, O.; Trzybiński, D.; Woźniak, K.; Osella, S.; Trzaskowski, B.; Grela, K. Azoliniums, Adducts, NHCs and Azomethine Ylides: Divergence in Wanzlick Equilibrium and Olefin Metathesis Catalyst Formation. *Chem.—A Eur. J.* **2018**, *24*, 4785–4789. [\[CrossRef\]](#)
39. Serra-Crespo, P.; Ramos-Fernandez, E.V.; Gascon, J.; Kapteijn, F. Synthesis and Characterization of an Amino Functionalized MIL-101(Al): Separation and Catalytic Properties. *Chem. Mater.* **2011**, *23*, 2565–2572. [\[CrossRef\]](#)
40. Rouquerol, J.; Llewellyn, P.L.; Rouquerol, F. Is the bet equation applicable to microporous adsorbents. *Stud. Surf. Sci. Catal.* **2007**, *160*, 49–56. [\[CrossRef\]](#)
41. Walton, K.S.; Snurr, R.Q. Applicability of the BET Method for Determining Surface Areas of Microporous Metal–Organic Frameworks. *J. Am. Chem. Soc.* **2007**, *129*, 8552–8556. [\[CrossRef\]](#)
42. Zwoliński, K.M.; Nowak, P.; Chmielewski, M.J. Towards multifunctional MOFs – transforming a side reaction into a post-synthetic protection/deprotection method. *Chem. Commun.* **2015**, *51*, 10030–10033. [\[CrossRef\]](#)
43. Ho, T.-L.; Olah, G.A. Cleavage of Esters and Ethers with Iodotrimethylsilane. *Angew. Chem. Int. Ed.* **1976**, *15*, 774–775. [\[CrossRef\]](#)

**Disclaimer/Publisher’s Note:** The statements, opinions and data contained in all publications are solely those of the individual author(s) and contributor(s) and not of MDPI and/or the editor(s). MDPI and/or the editor(s) disclaim responsibility for any injury to people or property resulting from any ideas, methods, instructions or products referred to in the content.